Transcriptomic study of high-glucose effects on human skin fibroblast cells

LINGXIA PANG[1*], YOUPEI WANG[2*], MEIQIN ZHENG[2], QING WANG[1], HONG LIN[3], LIQING ZHANG[4] and LINGJIAN WU[5]

[1]Function Experiment Teaching Center, Wenzhou Medical University, Wenzhou, Zhejiang 325305; [2]Clinical Examination Center, The Affiliated Eye Hospital, Wenzhou Medical University, Wenzhou, Zhejiang 325000; [3]Zhejiang Provincial Key Laboratory of Medical Genetics, Wenzhou Medical University, Wenzhou, Zhejiang 325035; [4]Operating Room; [5]Department of Dermatology, The First Affiliated Hospital of Wenzhou Medical University, Wenzhou, Zhejiang 325000, P.R. China

Received April 21, 2015; Accepted December 8, 2015

DOI: 10.3892/mmr.2016.4822

Abstract. Skin ulcers are a common complication of diabetes mellitus (DM). Fibroblasts are located within the dermis of skin tissue and can be damaged by diabetes. However, the underlying mechanism of how DM affects fibroblasts remains elusive. To understand the effects of DM on fibroblasts, the current study mimicked DM by high-glucose (HG) supplementation in the culture medium of human foreskin primary fibroblast cells, and the analysis of transcriptomic changes was conducted. RNA sequencing-based transcriptome analysis identified that, upon HG stress, 463 genes were upregulated and 351 genes downregulated (>1.5-fold changes; P<0.05). These altered genes were distributed into 20 different pathways. In addition, gene ontology (GO) analysis indicated that 31 GO terms were enriched. Among the pathways identified, nuclear factor κB (NF-κB) pathway genes were highly expressed, and the addition of Bay11-7082, a typical NF-κB signaling inhibitor, blocked the previously observed alterations in plasminogen activator inhibitor 1 (PAI1), an inflammation marker and frizzled class receptor 8 (FZD8), a Wnt signaling gene, expression that resulted from HG stress. Furthermore, an inhibitor of Wnt signaling diminished the role of Bay11-7082 in the regulation of PAI1 expression under HG conditions, suggesting that Wnt signaling may function downstream of the NF-κB pathway to protect fibroblast cells from HG stress. To the best of our knowledge, the current study is the first analysis of transcriptomic responses under HG stress in human fibroblasts. The data provided here may aid the understanding of the molecular mechanisms by which fibroblast cells are damaged in the skin of patients with DM.

Correspondence to: Professor Meiqin Zheng, Clinical Examination Center, The Affiliated Eye Hospital, Wenzhou Medical University, 268 Xueyuanxi Road, Wenzhou, Zhejiang 325000, P.R. China
E-mail: 35176404@qq.com

Professor Qing Wang, Function Experiment Teaching Center, Wenzhou Medical University, 268 Xueyuanxi Road, Wenzhou, Zhejiang 325305, P.R. China
E-mail: 33508598@qq.com

*Contributed equally

Key words: RNA-Seq, skin, high-glucose, fibroblasts, damage

Introduction

Diabetes mellitus (DM) is the most severe metabolic disease in the developed world, affecting a large number of people. A major symptom of DM is hyperglycemia, which leads to severe complications (1). Among patients with DM, ~15% exhibit impaired skin wound healing (2), and high blood sugar is linked to skin ulceration by altering angiogenesis (3), but the underlying mechanism remains unclear.

Skin wound repair requires the coordination of several cell types, including keratinocytes, fibroblasts, endothelial cells, macrophages and platelets. Fibroblast cell proliferation and migration, collagen deposition and remodeling, wound contraction and angiogenesis are important steps during wound repair (4,5). Extracellular matrix (ECM) forms the largest component of the dermal skin layer, therefore, the repair of damaged ECM is a key step for wound healing (6). Fibroblasts constitute one of the important cell layers that participate in the production and remodeling the ECM and fibroblast proliferation and migration are important for the formation of granulation tissue and further skin repair (7,8). The impaired wound healing during DM is attributed to altered protein and lipid metabolism and the associated abnormal formation of granulation tissue (9). Higher glucose levels in the blood result in abnormal attachment of aldose sugars to a protein or lipid, which affects normal glycosylation modifications (9). The aberrantly glycosylated products [advanced glycation end products (AGEs)] then accumulate in cells. AGEs attached to ECM proteins may lead to a reduction in their turnover rate (9). Nitric oxide (NO) is an important mediator of cell proliferation, maturation and differentiation and serves a key role in wound healing (10). Fibroblasts isolated from diabetic ulcers are usually large and widely

spread during *in vitro* culture compared with normal fibroblasts in age-matched controls. They often exhibit abnormal endoplasmic reticulum, increased numbers of vesicular bodies and lost microtubular structure. Therefore, DM affects protein turnover, autonomous trafficking and normal protein secretion in diabetic ulcer fibroblasts (11,12). Fibroblasts from diabetic ulcers have defects in cell proliferation, which may result in decreased ECM protein production and further delayed wound healing (13). High glucose-induced fibroblast migration was previously identified to be a result of reduced JNK activity (14). However, few molecular studies have investigating the underlying mechanisms of DM-mediated fibroblast cell damage.

In the present study, RNA sequencing (RNA-Seq) was used to analyze the alterations of large numbers of transcripts following HG stimulation of human fibroblast cells, and the genes and pathways associated with HG stress were identified. Additionally, the inflammatory response pathway and Wnt signaling were further analyzed for their role in the protection of fibroblasts from HG damage. The results of current study may be important for understanding the mechanisms of DM-mediated skin ulceration and may provide a theoretical basis for repair of skin damage in patients with DM in the future.

Materials and methods

Human foreskin fibroblast cell culture. Human fibroblast cells were isolated and subsequently cultured for analysis of the effects of HG treatment. All the procedures followed for purification and culture of human fibroblasts were described by Xuan *et al* (14). Human foreskin samples were collected from 3 patients in Department of Dermatology, the First Affiliated Hospital, Wenzhou Medical University (Wenzhou, China). This study was approved by the ethics committee of Wenzhou Medical University (Wenzhou, China) and written informed consent was obtained from all the patients involved. The fat was removed from the tissue and was cut into 3 by 2 mm strips and were incubated overnight at 4˚C in 0.05% Dispase I (Sigma-Aldrich, St. Louis, MO, USA). The epidermis was removed and the dermis was placed in 25-cm^2 flasks pre-treated with FBS, and placed horizontally for 1 h and then vertically for 3 h in a culture chamber with 5% CO_2 at 37˚C. The cells were cultured in Dulbecco's modified Eagle's medium (DMEM; HyClone; GE Healthcare Life Sciences, Logan, UT, USA) containing 5.5 mM glucose with 10% fetal bovine serum (FBS; HyClone; GE Healthcare Life Sciences) and 1% penicillin-streptomycin (Gibco; Thermo Fisher Scientific Inc., Watham, MA, USA) the medium was changed every 3 days. When cell confluence reached 70-80% the cells were digested and passaged with 0.25% trypsin (Gibco; Thermo Fisher Scientific Inc.) Cells were cultured for 3 days in 5.5 mM glucose medium and transferred to the media containing either 5.5 mM glucose (LG) or 30 mM glucose (HG). Cells at passage 3-6 were used for the LG and HG treatment. Cells were harvested after 1 h of LG and HG treatment.

Cell proliferation assay. Cell proliferation was assayed using a Cell Counting Kit-8 (CCK-8) kit (Dojindo Molecular Technologies, Inc., Kumamoto, Japan). The fibroblast cell culture and measurement of cell densities under different treatments were followed as previously described (14). In summary, 50 ml of the cell resuspension solution ($1x10^3$ cells/well) were transferred into 96-well plates following digestion with trypsin, and five parallel wells were used for each treatment. Subsequent to attachment to the culture plate, the cells were subjected to the different glucose treatments for 72 h in a 5% CO_2 incubator at 37˚C. Then, 5 ml of CCK-8 was added to each well, and the cells were cultured for another 3 h. Cell density was determined by quantifying the absorbance at 450 nm using a Varioskan Flash Multimode Reader (Thermo Fisher Scientific, Inc.) using the following formula: Cell density=$(A_{cell+CCK8+medium}-A_{CCK8+medium}/A_{cell+CCK8}-A_{CCK8+medium})$ x 100.

Table I. Reverse transcription-quantitative polymerase chain reaction primer sequences.

Primer	Sequence
Caspase 3	F: TGATGATGACATGGCGTGTC
	R: GTTGCCACCTTTCGGTTAAC
PAI1	F: GAGACTGAAGTCGACCTCAG
	R: CTGTCCATGATGATCTCCTC
GAPDH	F: GACCTGCCGTCTAGAAAAAC
	R: CTGTAGCCAAATTCGTTGTC
CCL13	F: CGTCCCATCTACTTGCTGCT
	R: TCAAGTCTTCAGGGTGTGAGC
IL8	F: GGTGCAGTTTTGCCAAGGAG
	R: TTCCTTGGGGTCCAGACAGA
FZD8	F: CTGGTGGAGATCCAGTGCTC
	R: TTGTAGTCCATGCACAGCGT
EGR2	F: TCGCAAGTACCCCAACAGAC
	R: CTCATCACTCCGGGCAAACT

PAI1, plasminogen activator inhibitor 1; GAPDH, glyceraldehyde-3-phosphate dehydrogenase; CCL13, chemokine (C-C motif) ligand 13; IL8, interleukin 8; FZD8, frizzled class receptor 8; EGR2, early growth response 2.

RNA deep sequencing. Total RNA was extracted from human foreskin fibroblasts for RNA-Seq experiments following treatment with a low (5.5 mM) or high (30 mM) concentration of glucose. RNA-Seq experiments and data analysis were performed by the NovelBio Bio-Pharm Technology Co., Ltd. (Shanghai, China). The RNA-Seq data is available upon request.

Analysis of the pathway and gene ontology (GO) category. Differentially expressed genes were identified by analyzing for association with biological process gene ontology (GO) terms (15). Fisher's exact test was used to classify the GO category, and the false discovery rate (FDR) was calculated to correct the P-value (16). Enrichment of GO members among differentially expressed gene sets was identified using the one-tailed Fisher's exact test for 2x2 contingency tables (17), which measures the significance of the function that as the enrichment increases, the corresponding function is more specific, which aids the identification of GOs with a more

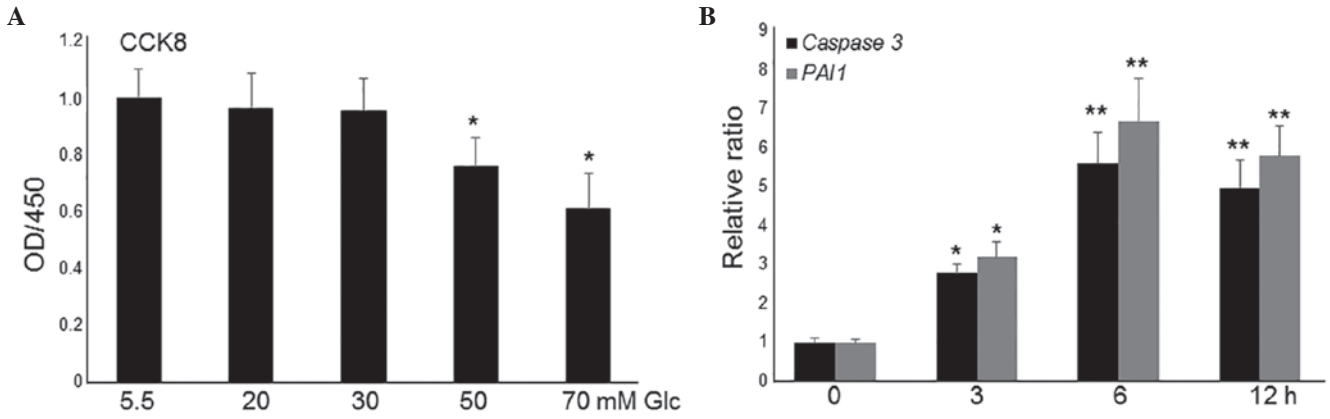

Figure 1. High-Glc effects on fibroblast cells. (A) Cell proliferation under the high-Glc conditions with 10% fetal bovine serum was measured by cell counting kit-8 assay after a 72-h incubation (*P<0.01 vs. the 5.5 mM Glc group; t-test). (B) Reverse transcription-quantitative polymerase chain reaction was performed to monitor the expression levels of caspase 3 and PAI1 following high-dose Glc (30 mM) treatment. GAPDH was used as an internal control. Data represent the mean ± standard error of 3 replicates. *P<0.05 and **P<0.01 vs. the 0 h group; t-test. Glc, glucose; OD, optical density; PAI1, plasminogen activator inhibitor 1.

concrete function description in the experiment. Pathway analysis was used to determine the significant pathways of the differential genes according to Kyoto Encyclopedia of Genes and Genomes (KEGG) (18), BioCarta (http://cgap.nci.nih.gov/Pathways/BioCarta_Pathways and Reactome(19).Fisher'sexacttestwasfollowedbyBenjamini-Hochberg multiple testing correction to select the significant pathway and the threshold of significance was defined by P-value and FDR (20).

Total RNA extraction, cDNA synthesis and reverse transcription-quantitative polymerase chain reaction (RT-qPCR). Total RNA was extracted from stimulated or unstimulated fibroblasts treated with high-concentration glucose (30 mM), Bay11-7082 (0.5 μM; Sigma-Aldrich) or inhibitor of Wnt response (IWR) (0.5 μM; Sigma-Aldrich). The cell monolayer was rinsed with ice-cold phosphate-buffered saline once. Each sample was treated with RQ1-DNAse (Promega Corporation, Madison, WI, USA). The cells were then lysed directly in a culture dish by adding 1 ml TRIzol (Thermo Fisher Scientific, Inc.) per each 3.5 cm diameter dish, scraped with a cell scraper and then 0.2 ml chloroform was added per 1 ml TRIzol. RNA (2 μg) was reverse transcribed at 42˚C for 60 min, 70˚C for 5 min and following stop the reaction at 8˚C using a GoScript Reverse Transcription System (Promega Corporation) following the manufacturer's protocol. A SYBR Green Master Mix (Bio-Rad Laboratories, Inc., Hercules, CA, USA) was used to perform the qPCR on an Illumina Eco 3.0 (Illumina, Inc., San Diego, CA, USA). A typical reaction consisted of an initial denaturation at 95˚C for 3 min, followed by 40 cycles of denaturation for 30 sec at 95˚C, annealing for 30 sec at 58˚C, and extension at 72˚C for 30 sec, followed by a final extension at 72˚C for 5 min. The transcription levels were normalized against those of GAPDH using the $2^{-\Delta\Delta Cq}$ method (21). The gene-specific primer sequences used for RT-qPCR are described in Table I. Each experiment was repeated at least 3 times. A unreversed transcribed RNA was used as a PCR template control.

Western blot analysis. For extraction of total protein, the cells were lysed in an ice-cold lysis solution containing 7 M urea, 2 Mthiourea, 2% CHAPS detergent, 40 mM Trizma base, 40 mM dithiothreitol, 1% protease inhibitor, the lysates were centrifuged for 15 min at 15,000 x g. All reagents were sourced from Sigma-Aldrich. The supernatant from each tube was moved to a new tube. The total proteins were separated on a 10% sodium dodecyl sulfate polyacrylamide gel electrophoresis gel (Sigma-Aldrich) at 100 V for 2 h following extraction. Then transferred onto Immobilon-P Transfer Membranes (Merck Millipore, Tokyo, Japan). The membranes were incubated in Tris-buffered saline containing 5% skimmed milk and 0.05% Tween-20 (EMD Milipore, Billerica, MA, USA) for 1-2 h and reacted with the corresponding primary antibodies at 4˚C overnight. The following primary antibodies were purchased from Abcam, all at dilution of 1:2,000 (Cambridge, MA, USA): p-IKBα (mouse monoclonal; cat no. 39A1431, reactivity - mouse, rat, cow, human), IKBα (rabbit polyclonal; cat no. ab7217; reactivity - mouse, rat, human) and GAPDH (mouse monoclonal; cat no. mAbcam 9484; reactivity - mouse, rat, rabbit, chicken, cow, dog, human, pig). The membranes were incubated for 1 h with an anti-mouse or polyclonal anti-rabbit horseradish peroxidase-linked secondary antibody (cat. no. 7074; 1:2,000; Cell Signaling Technology, Inc., Danvers, MA, USA).

Statistical analysis. Statistical calculations were performed with Prism 5 software package (GraphPad Software, Inc., La Jolla, CA, USA). Significant differences are expressed as the mean ± standard error. The comparison between two groups was analyzed by t-test. P<0.05 was considered to indicate a statistically significant difference.

Results

HG induces apoptosis and inflammatory responses in fibroblasts. To simulate diabetes, HG was utilized to study its effects on the fibroblasts (22). To analyze the effects of different concentrations of HG on fibroblasts, cell proliferation was monitored in different concentrations of glucose-containing media with 10% fetal bovine serum. HG treatment up to 30 mM did not markedly alter cell proliferation, whilst culture in 50 and 70 mM glucose significantly inhibited cell

Table II. GO classification.

GO ID	GO term	Enrichment	(-log2P)	Up/ downregulated
0071371	Cellular response to gonadotropin stimulus	19.12899	10.23295	Up
0034421	Post-translational protein acetylation	63.76331	9.872556	Up
0071320	Cellular response to cAMP	9.564497	9.733907	Up
0001508	Regulation of action potential	15.94083	9.562348	Up
0050890	Cognition	15.10184	9.362226	Up
0034088	Maintenance of mitotic sister chromatid cohesion	47.82249	9.297728	Up
0006642	Triglyceride mobilization	38.25799	8.822425	Up
0035356	Cellular triglyceride homeostasis	38.25799	8.822425	Up
0071356	Cellular response to tumor necrosis factor	7.501566	8.538068	Up
0042471	Ear morphogenesis	31.88166	8.417503	Up
0042158	Lipoprotein biosynthetic process	31.88166	8.417503	Up
0045444	Fat cell differentiation	6.596205	7.912633	Up
0048752	Semicircular canal morphogenesis	23.91124	7.753206	Up
0030728	Ovulation	23.91124	7.753206	Up
0006955	Immune response	2.610657	7.576953	Up
0006351	Transcription, DNA-templated	1.628693	7.526714	Up
0042472	Inner ear morphogenesis	5.710147	7.220235	Up
0010875	Positive regulation of cholesterol efflux	17.38999	6.989887	Up
0002237	Response to molecule of bacterial origin	17.38999	6.989887	Up
0006334	Nucleosome assembly	7.598543	21.94307	Down
0035115	Embryonic forelimb morphogenesis	12.5653	13.38364	Down
0007275	Multicellular organism development	2.149419	11.51722	Down
0032688	Negative regulation of interferon-beta production	53.61194	9.387513	Down
0060675	Ureteric bud morphogenesis	53.61194	9.387513	Down
2001181	Positive regulation of interleukin-10 secretion	53.61194	9.387513	Down
0048706	Embryonic skeletal system development	8.247991	8.969668	Down
0009952	Anterior/posterior pattern specification	4.684538	8.623385	Down
0060070	Canonical Wnt signaling pathway	5.154994	8.014638	Down
0010042	Response to manganese ion	26.80597	7.938039	Down
0009954	Proximal/distal pattern formation	10.05224	7.809469	Down
0046628	Positive regulation of insulin receptor signaling pathway	22.97655	7.587427	Down

GO, gene ontology.

proliferation compared with culture in low-glucose (LG; 5.5 mM; P<0.01; Fig. 1A). However, this concentration of glucose is much higher than the levels recorded in patients' blood; therefore, 20 and 30 mM were used to further analyze gene expressions. Compared to 30 mM, 20 mM of glucose did not significantly affect the expression levels of caspase 3 and PAI1 (data not shown). Therefore, 30 Mm of glucose was selected for transcriptome analysis. As presented in Fig. 1A, 30 mM glucose treatment did not affect cell proliferation activity, thus, the expression levels of two apoptosis and inflammation marker genes, caspase 3 and plasminogen activator inhibitor 1 (PAI1), were further monitored at this concentration. RT-qPCR results indicated that the application of 30 mM glucose led to an increase in the expression levels of caspase 3 and PAI1 following 3-h treatment, which reached a peak at 6 h (Fig. 1B). These data indicate that HG culture damages fibroblast cells.

Identification of HG-regulating transcriptome in fibroblasts. To identify HG-regulated genes and pathways, RNA-Seq experiments were performed using human fibroblast cells cultured in LG (5.5 mM) and HG (30 mM). Since Caspase 3 and PAI1 expression levels were highest at 6 h subsequent to HG stress, the fibroblast cells stimulated for 6 h with LG and HG were collected for RNA-Seq analysis. The RNA-Seq results demonstrated that 814 genes were differentially expressed (>1.5-fold change; P<0.05) in the HG-treated fibroblasts compared with LG-treated cells. Among them, 351 genes were downregulated, and 463 genes were upregulated (Fig. 2A), determined from statistical outcomes by analysis for association with biological process GO terms. To verify the RNA-Seq data, HG-mediated expression levels of the following four genes were assessed by RT-qPCR: Interleukin 8 (IL8), chemokine (C-C motif) ligand 13 (CCL13), frizzled class receptor 8 (FZD8) and early growth receptor 2

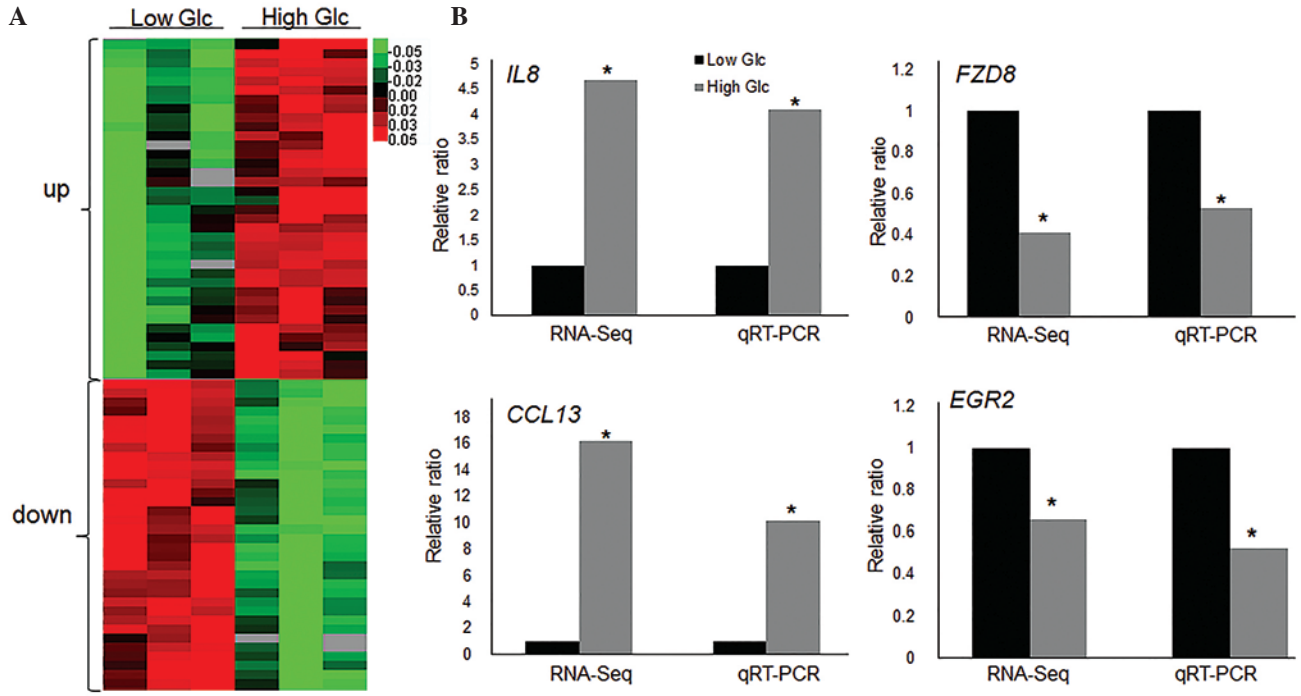

Figure 2. High Glc regulated transcriptome profile. (A) Heat map represents the differentially expressed genes following high Glc (30 mM) treatment for 6 h in human fibroblast cells. Low Glc treatment was 5.5 mM. Gene expression is presented as a pseudocolor scale with red denoting higher gene expression levels and green denoting lower levels. Significant differences between low and high glucose treated groups were compared (P<0.05). (B) RT-qPCR was performed to verify the expression levels of IL8, CCL13, FZD8 and EGR2 and the data was compared with RNA-Seq results. Significant differences of IL8, FZD8, CCL13 and EGR2 expression levels between low and high glucose treated groups in both RNA-Seq and qRT-PCR analyses (*P<0.05) GAPDH was used as an internal control. Glc, glucose; RT-qPCR, reverse transcription-quantitative polymerase chain reaction; IL8, interleukin 8; FZD8, frizzled class receptor 8; CCL13, chemokine (C-C motif) ligand 13; EGR2, early growth response 2; RNA-Seq, RNA sequencing.

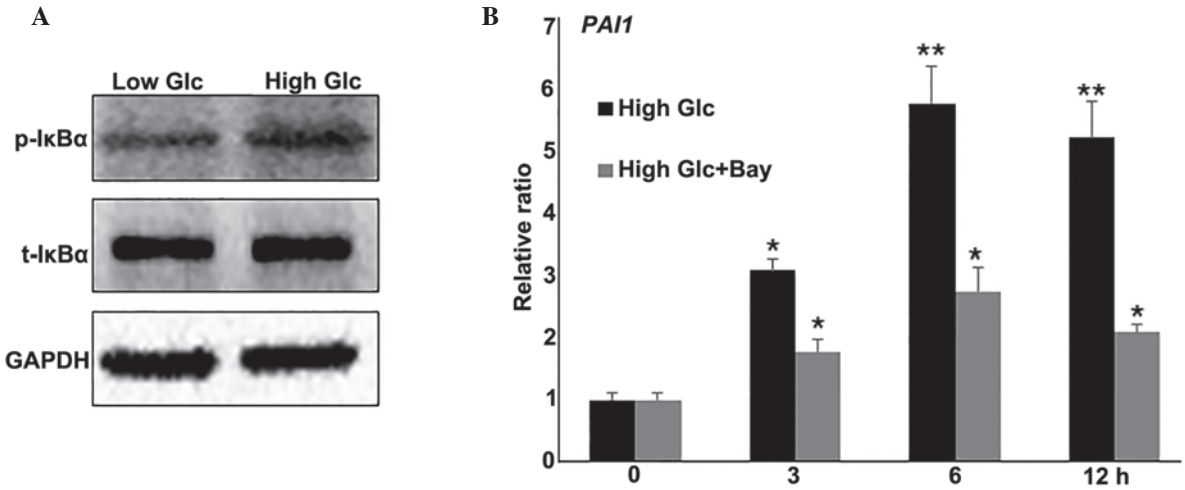

Figure 3. Role of the NF-κB pathway in high Glc-induced cell damage. (A) Western blot analysis was performed to analyze levels of p-IκBα and t-IκBα following high Glc stress for 1 h. (B) Reverse transcription-quantitative polymerase chain reaction was performed to monitor the expression levels of PAI1 following high Glc or high Glc + Bay (0.5 μM) treatment. GAPDH was used as an internal control. Data represent the mean ± standard error of 3 replicates. *P<0.05 and **P<0.01 vs. 0 h, t-test. NF-κB, nuclear factor κB; IκBα, NF-κB inhibitor α; p, phospho; t, total; Glc, glucose; Bay, Bay11-7082; PAI1, plasminogen activator inhibitor 1.

(EGR2). The inflammatory response genes (IL8 and CCL13) were upregulated, while the Wnt signaling gene (FZD8) and putative SUMO E3 ligase (EGR2) were repressed by HG stimulation, and the RT-qPCR results were similar to RNA-Seq data (Fig. 2B). GO analysis indicated that 31 GO terms were enriched (P<0.01; Table II). These genes were associated with multiple biological processes, including cellular triglyceride homeostasis, positive regulation of cholesterol efflux, the canonical Wnt signaling pathway and transcription (Table II). Further pathway analysis was performed with 814 genes that were altered by HG stress. The results demonstrated that these genes were divided into 20 different pathways, including NF-κB, tumor necrosis factor (TNF), Wnt, ECM/receptor interaction and hedgehog signaling pathways. Among them,

Table III. Pathway classification.

Pathway ID	Pathway term	Enrichment	(-log2P)	Up/ downregulated
05034	Alcoholism	8.39875	32.3993	Up
05322	Systemic lupus erythematosus	9.129076	29.151	Up
05217	Basal cell carcinoma	7.635227	10.23381	Up
04512	ECM-receptor interaction	4.772017	7.471521	Up
04916	Melanogenesis	4.157797	6.698221	Up
04390	Hippo signaling pathway	3.27224	6.165099	Up
05203	Viral carcinogenesis	2.840157	5.914846	Up
05202	Transcriptional misregulation in cancer	2.799583	5.229064	Up
04910	Insulin signaling pathway	2.957306	4.892077	Up
04340	Hedgehog signaling pathway	4.49933	4.869559	Up
04977	Vitamin digestion and absorption	6.998958	4.700239	Up
04064	NF-κB signaling pathway	6.15293	8.938564	Up
04668	TNF signaling pathway	5.090152	7.82519	Up
04060	Cytokine-cytokine receptor interaction	3.803208	9.593708	Down
04310	Wnt signaling pathway	2.74469	4.521127	Down
05202	Transcriptional misregulation in cancer	3.732778	6.955703	Down
05166	HTLV-I infection	2.94693	6.11439	Down
04621	NOD-like receptor signaling pathway	5.418548	5.528479	Down
05132	*Salmonella* infection	3.952353	4.424635	Down
05161	Hepatitis B	3.068037	4.341831	Down

ECM, extracellular matrix; NF-κB, nuclear factor κB; TNF, tumor necrosis factor; HTLV-I, human T-lymphotropic virus 1; NOD, nucleotide-binding oligomerization domain.

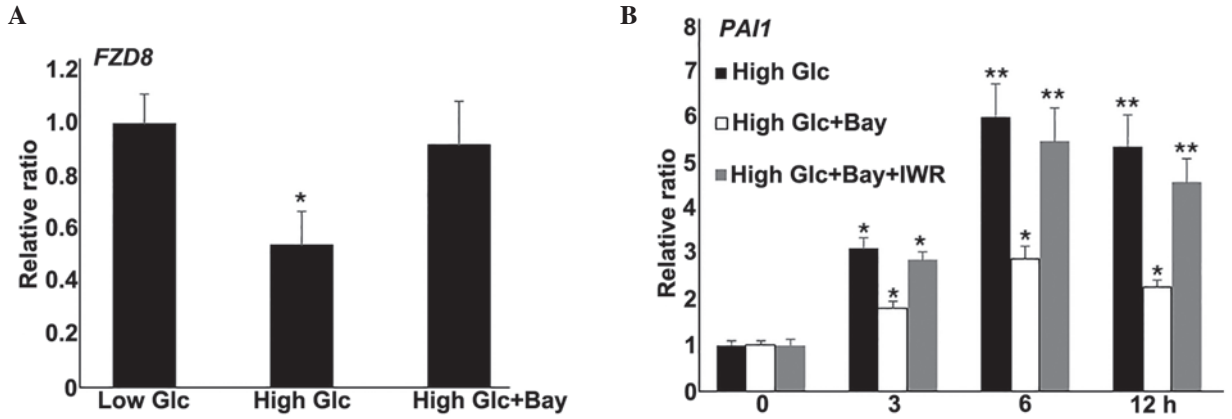

Figure 4. Effect of Wnt signaling pathway on high Glc-mediated cell damage. (A) RT-qPCR was performed to analyze expression level of Wnt signaling gene FZD8 after high Glc and high Glc + Bay treatment. *P<0.05 vs. low Glc; t-test. (B) RT-qPCR analysis for monitoring PAI1 expressions after Bay or Bay + IWR (a typical Wnt signaling inhibitor treatment) at the indicated time points. *P<0.05 and **P<0.01 vs. 0 h; t-test. Glc, glucose; RT-qPCR, reverse transcription-quantitative polymerase chain reaction; FZD8, frizzled class receptor 8; Bay, Bay11-7082; PAI1, plasminogen activator inhibitor 1; IWR, inhibitor of Wnt response.

certain inflammatory response pathways involving NF-κB and TNF were upregulated by HG stress, while Wnt signaling genes were downregulated (Table III). Together, these data indicate that HG regulates a large number of genes involved in various biological processes.

Regulatory role of the inflammatory response in HG-mediated fibroblast cell damage. The NF-κB pathway was identified to be involved in HG-regulated biological processes, the effect of the inflammatory response in HG-mediated fibroblast cell damage was further examined. To further evaluate the effects of HG on NF-κB signaling, the activity of IκBα, the most characterized and studied NF-κB regulator, was examined. IκBα is phosphorylated by IκB kinases (IKK), resulting in the translocation of NF-κB to the nucleus and transcription of target genes (23). Western blot analysis

indicated that HG induced IκBα phosphorylation (p-IκBα), but did not change total IκBα (t-IκBα) levels (Fig. 3A). To further analyze the effect of the inflammatory response on HG-mediated gene expression, a combination of HG stress and Bay11-7082 (0.5 μM), a representative NF-κB pathway inhibitor, was used to treat fibroblasts. RNA was extracted and RT-qPCR was performed to monitor PAI1 gene expression. The results indicated that HG induced an increase in PAI1 mRNA levels at 3 ($P<0.05$), 6 and 12 h ($P<0.01$) compared with the levels observed at 0 h, and this induction was blocked by inhibiting NF-κB with Bay11-7082 (Fig. 3B). Taken together, these results suggest that the inflammatory response is inversely correlated with HG-regulated gene expression.

Wnt signaling is downstream of the NF-κB pathway. Wnt signaling is known to regulate diverse aspects of numerous biological processes (24). The RNA-Seq data from the present study demonstrated repressed expression of a number of Wnt signaling genes following HG stimulation in fibroblasts. NF-κB pathway inhibition partially rescued HG-mediated fibroblast damage. Therefore, the relationship between NF-κB and Wnt signaling were investigated further. In the fibroblast cells stimulated with Bay11-7082 (0.5 μM) and HG, expression levels of the Wnt signaling gene, FZD8, were similar to the levels in the LG cells ($P>0.05$; Fig. 4A). To further evaluate the role of Wnt signaling in HG-mediated gene expression, IWR, a typical Wnt signaling inhibitor, was also used to treated fibroblasts alongside Bay11-7082 and HG culture, then PAI1 gene expression was measured. Notably, IWR application reduced the effect of Bay11-7082 on HG-induced PAI1 expression levels (Fig. 4B). Together, these data demonstrate that NF-κB inhibition blocked the gene expression changes induced by HG. Additionally, Wnt signaling inhibition reversed Bay11-7082-mediated PAI1 repression under HG conditions.

Discussion

Fibroblasts are important for synthesizing ECM and collagen, the structural framework (stroma) for skin tissues, and serve a key role in wound healing (25). Skin wound healing requires the involvement of several cell types, including keratinocytes, fibroblasts, endothelial cells, macrophages and platelets (26). Therefore, understanding the underlying mechanisms by which fibroblast cells protect themselves from DM is important for the treatment of skin ulcers (4). One of the strategies that all living organisms utilize to adapt to environmental changes is the rapid reprogramming of transcriptional regulations via cell signaling mechanisms (27-29). Therefore, analysis of transcriptomic changes under certain stress is a method to clarify the regulation of these mechanisms. In the present study, RNA-Seq was utilized to analyze transcriptomes, providing an efficient experimental basis to extract information regarding gene expression, somatic mutations and novel gene fusions (30) using HG-cultured human primary fibroblast cells. The results demonstrated a large population of differentially expressed genes following HG stimulation. Among them, 351 genes were downregulated and 463 were upregulated. Further, analyses of the associated pathways using GO and KEGG databases revealed various biological processes and pathways (Tables II and III).

ECM synthesis is important for skin wound repair. Various genes involved in ECM/receptor interactions were identified as undergoing changes in expression levels following HG stress (data available upon request). Other pathways identified to be altered by HG include NF-κB, TNF, Wnt, Hedgehog and Hippo signaling. The Wnt signaling pathway and fibroblast growth factor (FGF) regulate T-box family transcription factors, control cell fate within the zebrafish tailbud and are involved in axis elongation (31); FGF positively regulates Hedgehog signaling during embryonic tracheal cell migration (32); Hippo signaling and EGFR pathways control growth and activate tumorigenesis when dysregulated. Epidermal growth factor receptor (EGFR) activates Yorkie, a key Hippo pathway transcription factor that has been indicated to influence cell proliferation in Drosophila (33); and bFGF previously inhibited TNF-mediated activation of NF-κB by blocking phosphorylation and degradation of IκBα, leading to the repression of leukocyte adhesion in tumor vessels (34). HG has been demonstrated to affect FGF and downstream JNK activity, resulting in delay to human fibroblast cell migration (14). Therefore, those pathways that are regulated by HG may be partially connected to FGF signaling, which is known to accelerate DM-induced skin wound repair. Further biochemical and molecular studies are required to specify how these pathways are connected.

In the current study, inhibition of the NF-κB pathway through treatment with Bay11-7082 repressed the HG-induced PAI1 levels, suggesting that HG stimulation may activate inflammatory response pathways and cause damage to cells. Notably, Bay11-7082 application reversed the repression of FZD8 expression levels resulting from HG stress.

In addition, treatment with the Wnt signaling inhibitor, IWR, together with Bay11-7082 diminished the effects of Bay11-7082 on PAI1 repression under HG conditions, indicating that Wnt signaling functions downstream of the NF-κB pathway to regulate HG-mediated gene expression. HG stress negatively and positively regulated the NF-κB and Wnt signaling pathways, respectively, and this suggests that Wnt activation is important for the protection of fibroblasts from DM. The present study demonstrated HG-regulated gene expression in fibroblasts, and a link between the NF-κB pathway and Wnt signaling. In the future, these findings may be notable for the treatment of DM-induced skin ulcers.

Acknowledgements

The present study was made possible by an initiative grant from Wenzhou Medical University (Wenzhou, China).

References

1. Brownlee M: Biochemistry and molecular cell biology of diabetic complications. Nature 414: 813-820, 2001.
2. Yach D, Stuckler D and Brownell KD: Epidemiologic and economic consequences of the global epidemics of obesity and diabetes. Nat Med 12: 62-66, 2006.
3. Braiman-Wiksman L, Solomonik I, Spira R and Tennenbaum T: Novel insights into wound healing sequence of events. Toxicol Pathol 35: 767-779, 2007.
4. Martin P: Wound healing - aiming for perfect skin regeneration. Science 276: 75-81, 1997.

5. Gurtner GC, Werner S, Barrandon Y and Longaker MT: Wound repair and regeneration. Nature 453: 314-321, 2008.
6. Brem H and Tomic-Canic M: Cellular and molecular basis of wound healing in diabetes. J Clin Invest 117: 1219-22, 2007.
7. Wagner W and Wehrmann M: Differential cytokine activity and morphology during wound healing in the neonatal and adult rat skin. J Cell Mol Med 11: 1342-1351, 2007.
8. Kanazawa S, Fujiwara T, Matsuzaki S, Shingaki K, Taniguchi M, Miyata S, Tohyama M, Sakai Y, Yano K, Hosokawa K and Kubo T: bFGF regulates PI3-kinase-Rac1-JNK pathway and promotes fibroblast migration in wound healing. PLoS One 5: e12228, 2010.
9. Goldin A, Beckman JA, Schmidt AM and Creager MA: Advanced glycation end products: Sparking the development of diabetic vascular injury. Circulation 114: 597-605, 2006.
10. Obayashi K, Akamatsu H, Okano Y, Matsunaga K and Masaki H: Exogenous nitric oxide enhances the synthesis of type I collagen and heat shock protein 47 by normal human dermal fibroblasts. J Dermatol Sci 41: 121-126, 2006.
11. Loots MA, Lamme EN, Mekkes JR, Bos JD and Middelkoop E: Cultured fibroblasts from chronic diabetic wounds on the lower extremity (non-insulin-dependent diabetes mellitus) show disturbed proliferation. Arch Dermatol Res 291: 93-99, 1999.
12. Rowe DW, Starman BJ, Fujimoto WY and Williams RH: Abnormalities in proliferation and protein synthesis in skin fibroblast cultures from patients with diabetes mellitus. Diabetes 26: 284-290, 1977.
13. Bachschmid MM, Xu S, Maitland-Toolan KA, Ho YS, Cohen RA and Matsui R: Attenuated cardiovascular hypertrophy and oxidant generation in response to angiotensin II infusion in glutaredoxin-1 knockout mice. Free Radic Bio Med 49: 1221-1229, 2010.
14. Xuan YH, Huang BB, Tian HS,Chi LS, Duan YM, Wang X, Zhu ZX, Cai WH, Zhu YT, Wei TM, *et al*: High-glucose inhibits human fibroblast cell migration in wound healing via repression of bFGF-regulating JNK phosphorylation. PLoS One 9: e108182, 2014.
15. Gene Ontology Consortium: The gene ontology (GO) project in 2006. Nucleic Acids Res 34: D322-D326, 2006.
16. Dupuy D, Bertin N, Hidalgo CA, Venkatesan K, Tu D, Lee D, Rosenberg J, Svrzikapa N, Blanc A, Carnec A, *et al*: Genome-scale analysis of in vivo spatiotemporal promoter activity in *Caenorhabditis elegans*. Nat Biotechnol 25: 663-668, 2007.
17. Dunnick JK, Brix A, Cunny H, Vallant M and Shockley KR: Characterization of polybrominated diphenyl ether toxicity in Wistar Han rats and use of liver microarray data for predicting disease susceptibilities. Toxicol Pathol 40: 93-106, 2012.
18. Kanehisa M and Goto S: KEGG: Kyoto Encyclopedia of Genes and Genomes. Nucleic Acids Res 28: 27-30, 2000.
19. Matthews L, Gopinath G, Gillespie M, Caudy M, Croft D, de Bono B, Garapati P, Hemish J, Hermajakob H, Jassal B, *et al*: Reactome knowlegdebase of human biological pathways and processes. Nucleic Acids Res 37: 619-622, 2009.
20. Draghici S, Khatri P, Tarca AL, Amin K, Done A, Voichita C, Georgescu C and Romero R: A systems biology approach for pathway level analysis. Genome Res 17: 1537-1545, 2007.
21. Livak KJ and Schmittgen TD: Analysis of relative gene expression data using real-time quantitative PCR and the 2(-Delta Delta C(T)) method. Methods 25: 402-408, 2001.
22. Lamers ML, Almeida ME, Vicente-Manzanares M, Horwitz AF and Santos MF: High glucose-mediated oxidative stress impairs cell migration. PLoS One 6: e22865, 2011.
23. Baeuerle PA: IkappaB-NF-kappaB structures: At the interface of inflammation control. Cell 95: 729-731, 1998.
24. Malinauskas T and Jones EY: Extracellular modulators of Wnt signalling. Curr Opin Struct Biol 29: 77-84, 2014.
25. Krafts KP: Tissue repair: The hidden drama. Organogenesis 6: 225-233, 2010
26. Hinz B: Masters and servants of the force: The role of matrix adhesions in myofibroblast force perception and transmission. Eur J Cell Biol 85: 175-181, 2006.
27. Greenhalgh DG: The role of apoptosis in wound healing. Int J of Biochem Cell Biol 30: 1019-1030, 1998.
28. Stashak TS, Farstvedt E and Othic A: Update on wound dressings: Indications and best use. Clin Tech Equine Prac 3: 148-163, 2004.
29. Versteeg HH, Heemskerk JW, Levi M and Reitsma PH: New fundamentals in hemostasis. Physiological Reviews 93: 327-358, 2013.
30. Meyerson M, Gabriel S and Getz G: Advances in understanding cancer genomes through second-generation sequencing. Nat Rev Genet 11: 685-696, 2010.
31. Stulberg MJ, Lin A, Zhao H and Holley SA: Crosstalk between Fgf and Wnt signaling in the zebrafish tailbud. Dev Biol 369: 298-307, 2012.
32. Butí E, Mesquita D and Araújo SJ: Hedgehog is a positive regulator of FGF signalling during embryonic tracheal cell migration. PLoS One 9: e92682, 2014.
33. Reddy BV and Irvine KD: Regulation of Hippo signaling by EGFR-MAPK signaling through Ajuba family proteins. Dev Cell 24: 459-471, 2013.
34. Flati V, Pastore LI, Griffioen AW, Satijn S, Toniato E, D'Alimonte I, Laglia E, Marchetti P, Gulino A and Martinotti S: Endothelial cell anergy is mediated by bFGF through the sustained activation of p38-MAPK and NF-kappaB inhibition. Int J Immunopathol Pharmacol 19: 761-773, 2006.